



The RIC H Detector of the AMS-02 experiment aboard the International Space Station

*F. Giovacchini - CIEMAT
on behalf of the AMS-02 Collaboration*

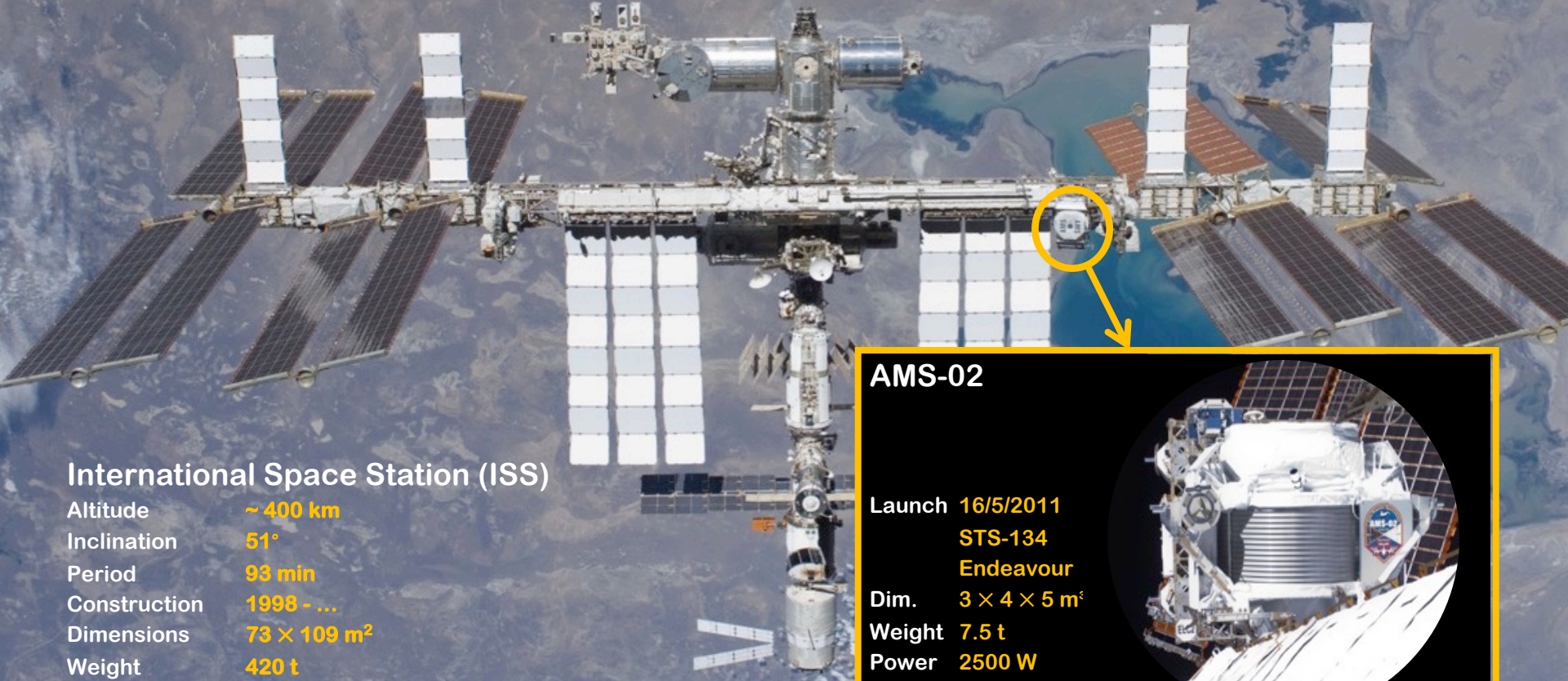
13/09/2022, Edinburgh

F. Giovacchini - CIEMAT

RIC H 2022

The Alpha Magnetic Spectrometer

Installed in 2011 on the ISS. Takes data continuously since then.
AMS-02 collected more than **200 billion cosmic rays** up to now.
It is expected to take data during the whole ISS lifetime (2030).



International Space Station (ISS)

Altitude	~ 400 km
Inclination	51°
Period	93 min
Construction	1998 - ...
Dimensions	73 × 109 m ²
Weight	420 t

AMS-02

Launch	16/5/2011
	STS-134
	Endeavour
Dim.	3 × 4 × 5 m ³
Weight	7.5 t
Power	2500 W



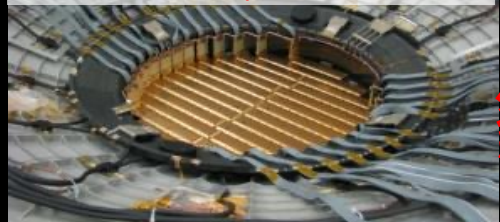
AMS: a high energy physics detector in space

Particles and nuclei are defined by their charge (Z) and energy ($E \sim p$)

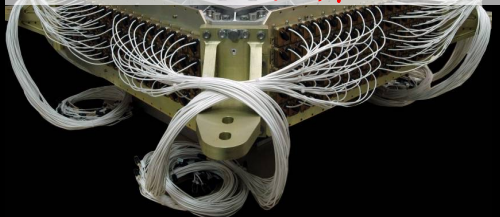
Transition Radiation Detector (TRD)
identify e^+ , e^-



Silicon Tracker
 Z, P



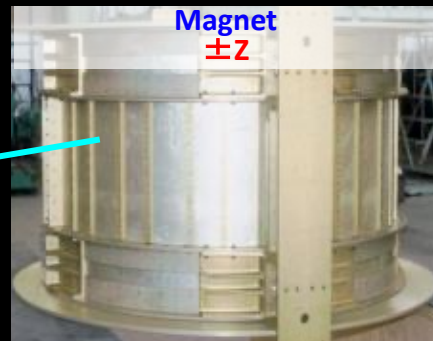
Electromagnetic Calorimeter (ECAL)
 E of e^+ , e^- , γ



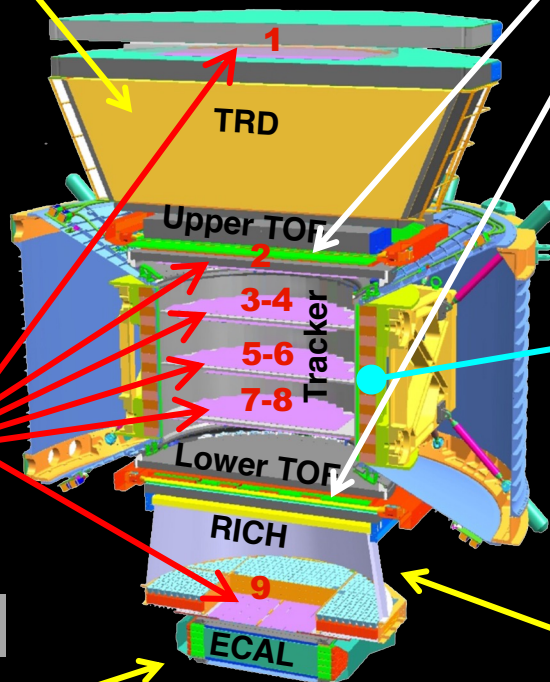
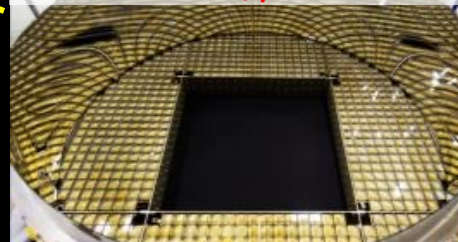
Upper & Lower TOF
 Z, β



Magnet
 $\pm Z$

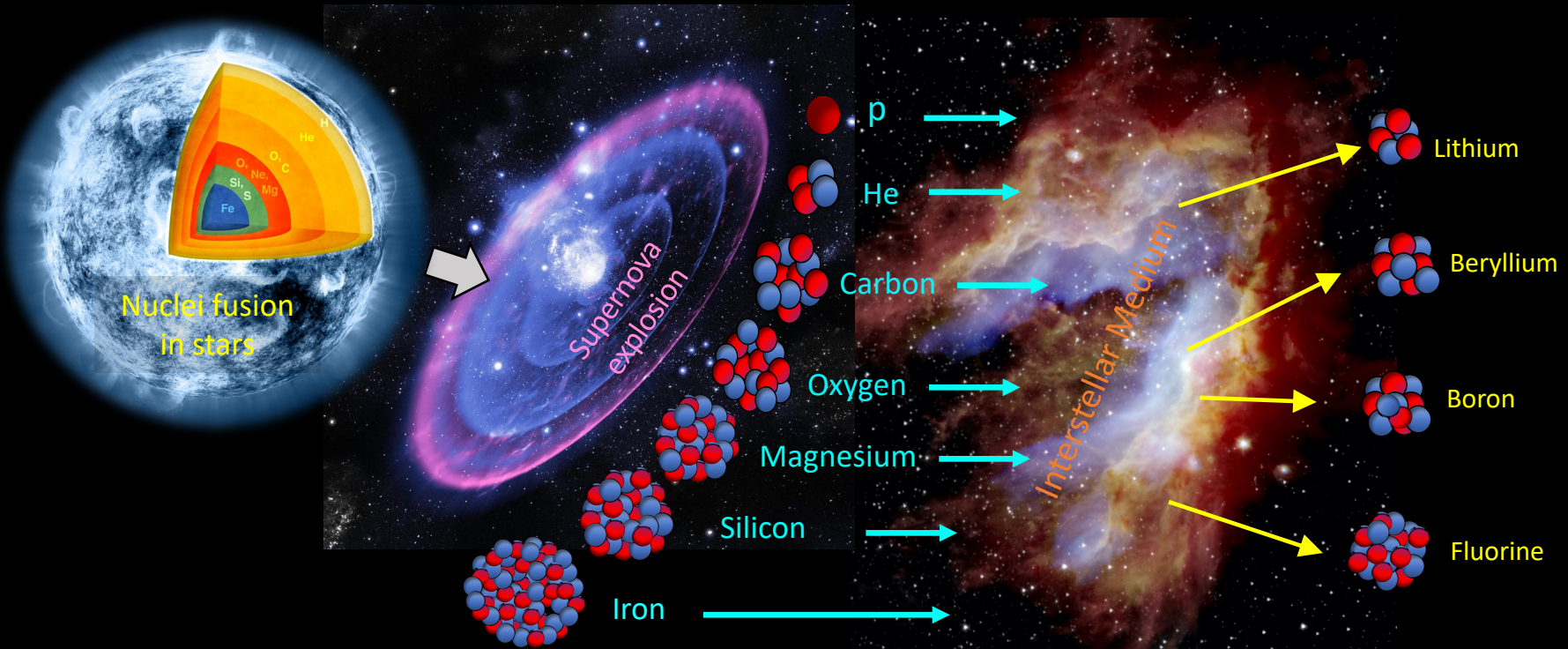


Ring Imaging Cerenkov (RICH)
 Z, β



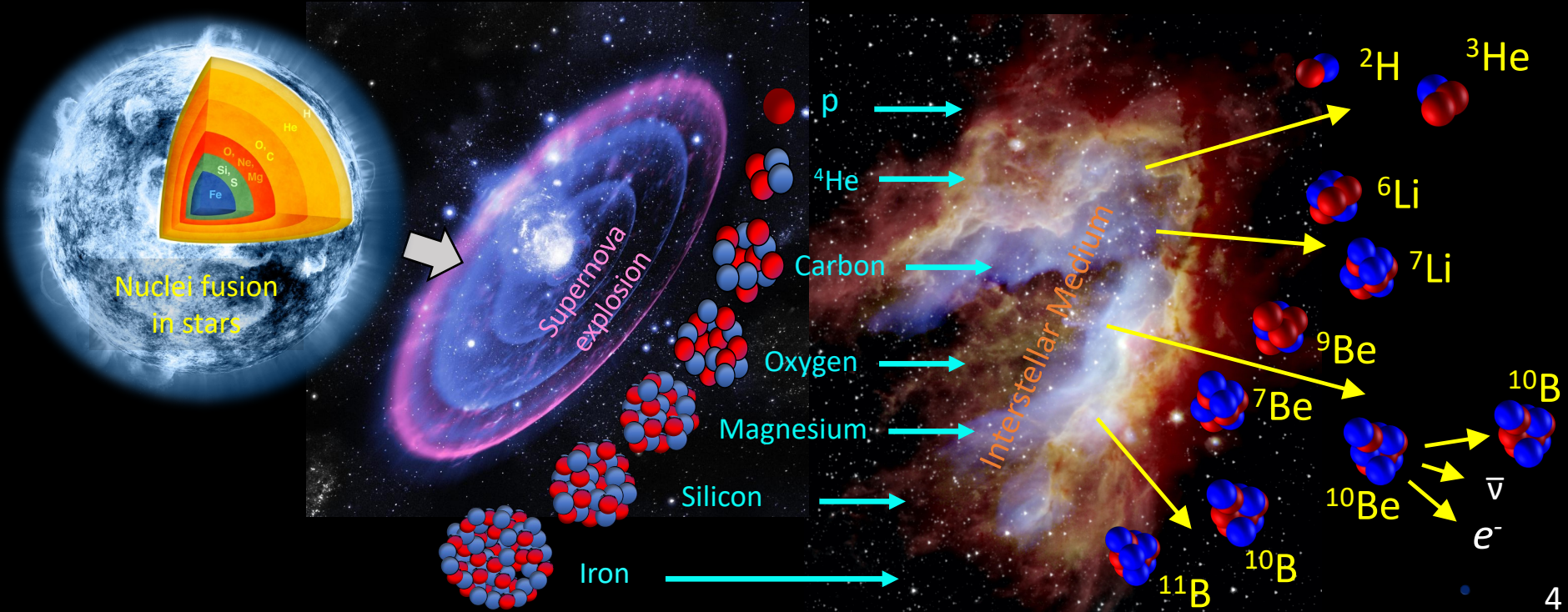
AMS: Physics goals

- Search for Anti Matter ($\bar{\text{He}}$) and Dark Matter hints in our galaxy as excess on rare CRs components (like positrons, \bar{p} , \bar{d}) above the expected astrophysical background;
- Precise measurement of **primary** and **secondary** cosmic ray spectra: fundamental to understand the origin, acceleration and propagation of Cosmic Rays in our Galaxy.

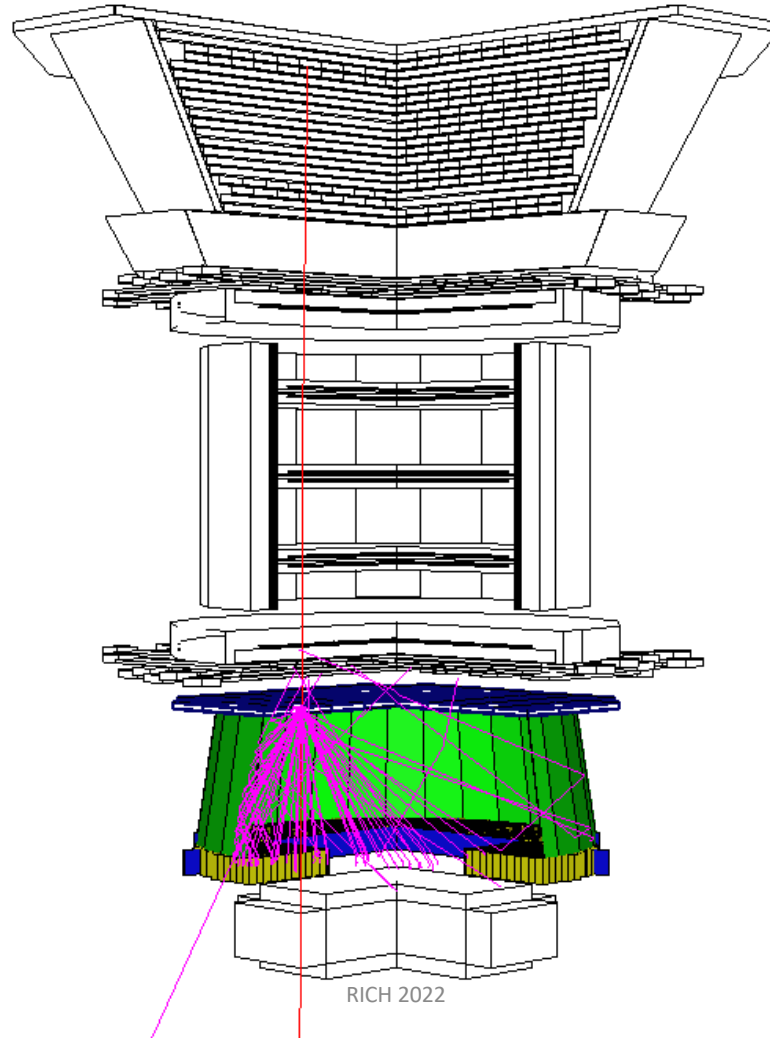


AMS: Physics goals

- Search for Anti Matter ($\bar{\text{He}}$) and Dark Matter hints in our galaxy as excess on rare CRs components (like positrons, \bar{p} , \bar{d}) above the expected astrophysical background;
 - Precise measurement of **primary** and **secondary** cosmic ray spectra: fundamental to understand the origin, acceleration and propagation of Cosmic Rays in our Galaxy.
- A more detailed insight from isotopic composition of light nuclei (D , ${}^3\text{He}$, ${}^4\text{He}$, ${}^6\text{Li}$, ${}^7\text{Li}$, ${}^7\text{Be}$, ${}^9\text{Be}$, ${}^{10}\text{Be}$)

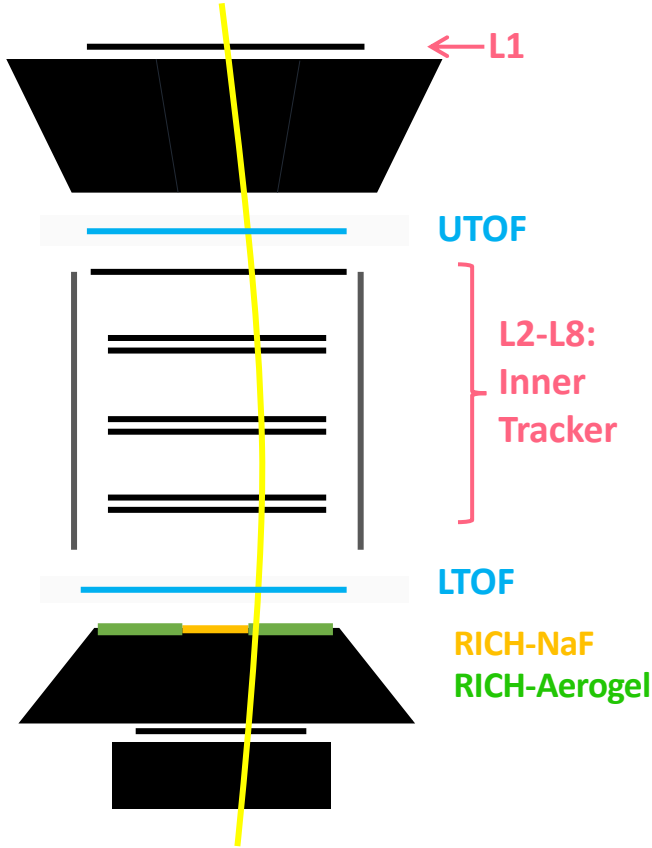


The AMS Ring Imaging Cherenkov detector



RICH 2022

Isotopes identification in AMS



$$M = \frac{RZ}{\beta\gamma}$$

$$\frac{\Delta M}{M} = \sqrt{\left(\frac{\Delta R}{R}\right)^2 + \left(\gamma^2 \frac{\Delta\beta}{\beta}\right)^2}$$

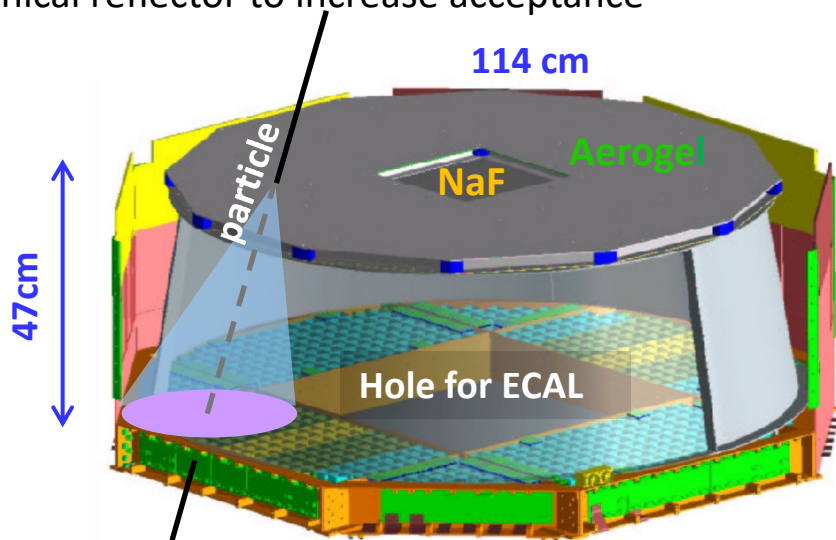
- Charge measurement:
Tracker layers, UTOF, LTOF, RICH
- Rigidity= p/Z measurement :
Tracker, $\Delta R/R \sim 10\%$ at 10 GV
- β measurements: **TOF, RICH-NaF, RICH-Aerogel**

	E_{kn} range (GeV/n)	$\Delta\beta/\beta$	
		(Z=2, $\beta=1$)	(Z=4, $\beta=1$)
TOF	(0.5, 1.2)	$\sim 2\%$	$\sim 1.5\%$
RICH-NaF ($n=1.33$)	(0.8, 4.0)	$\sim 0.25\%$	$\sim 0.15\%$
RICH-Agl ($n=1.05$)	(3.0, 12)	$\sim 0.07\%$	$\sim 0.05\%$

The AMS-02 RICH: Detector Layout

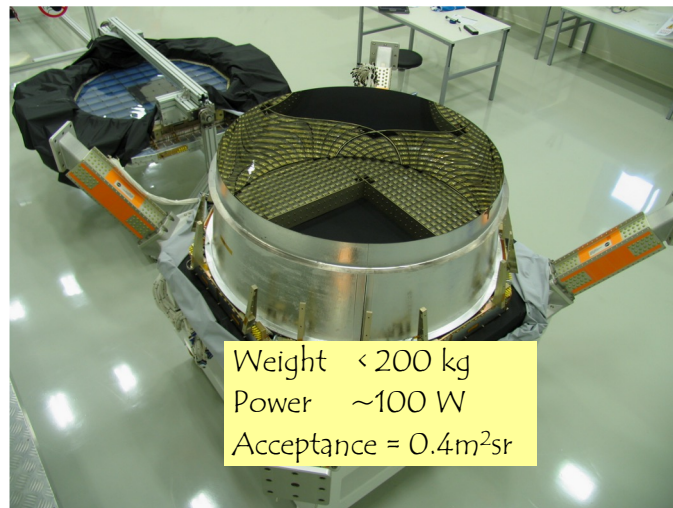
Proximity Focusing detector with:

- Dual radiator configuration
- Detection matrix with central hole (match ECAL)
- Conical reflector to increase acceptance

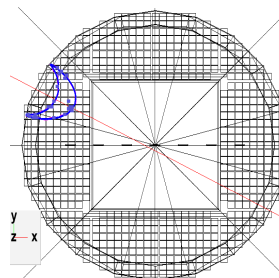


$\ominus \rightarrow v$
Intensity $\rightarrow Z^2$

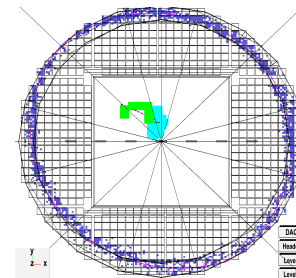
- Tracker inner track provide the entry point and direction
- On average one ring per event is reconstructed



$Z = 2$ (${}^3\text{He}$)
 $P = 19\text{GeV}/c$



$Z = 26$ (Fe)
 $P = 167\text{ GeV}/c$



The AMS-02 RICH: Radiator



92 AgI tiles ($n=1.05$)

Catalysis Institute of Novosibirsk

Refraction index	1.05
Δn among different tiles	≤ 0.001
Thickness (mm)	25
Size (mm ²)	113 x 113
Clarity (mm ⁴ /cm)	0.0055
Opening Angle at $\beta \rightarrow 1$ (deg)	17.8
Threshold velocity	0.952

16 NaF ($n=1.33$)

SODIUM FLUORIDE

Refraction index	1.33
Thickness (mm)	5
Size (mm ²)	85 x 85
Opening Angle at $\beta \rightarrow 1$ (deg)	41.5
Threshold velocity	0.752

NaF radiator:

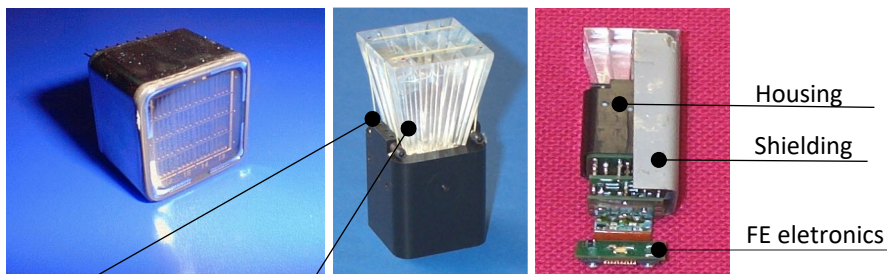
- Cover the energy range gap between TOF and agI;
- Larger Cherenkov angle ($D \text{ ring}_{\text{NaF}} \approx 85 \text{ cm} - D \text{ ring}_{\text{AgI}} \approx 31 \text{ cm}$ for $\beta \rightarrow 1$) allows to recover detection efficiency for central particle;

The AMS-02 RICH: Detection plane

Detection plane:

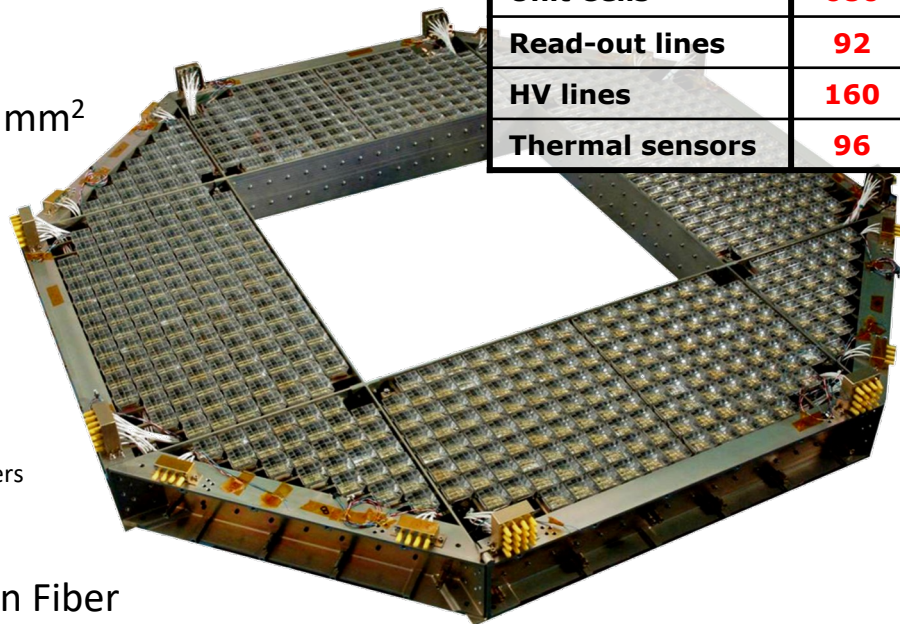
680 PMT Hamamatsu R7900-M16 (multianode 4x4)

10880 channels with detection granularity of $8.5 \times 8.5 \text{ mm}^2$



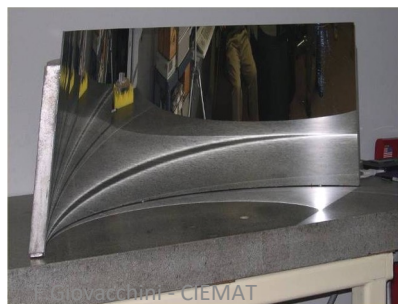
Kevlar wire fixation / Light guide: Diakon LG-70, acrylic plastic free of UV absorbers

Unit Cells	680
Read-out lines	92
HV lines	160
Thermal sensors	96



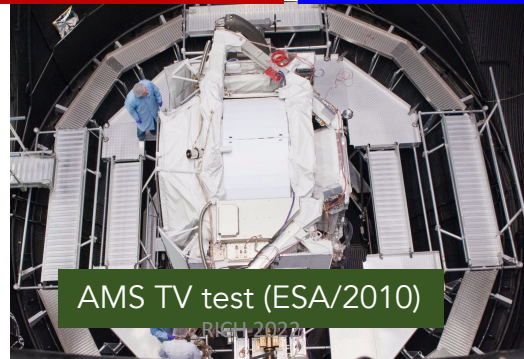
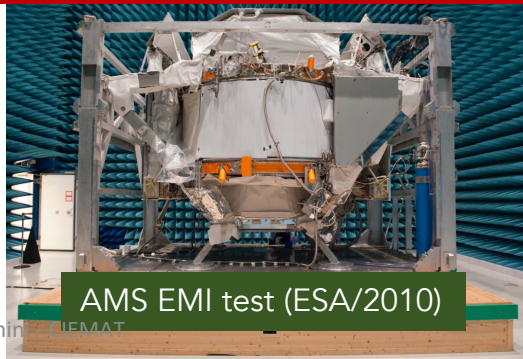
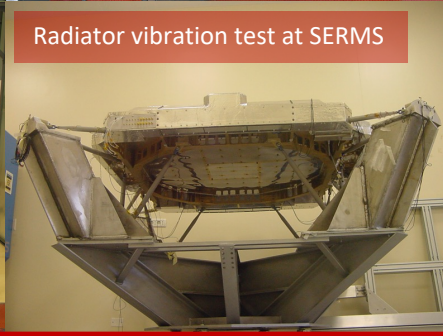
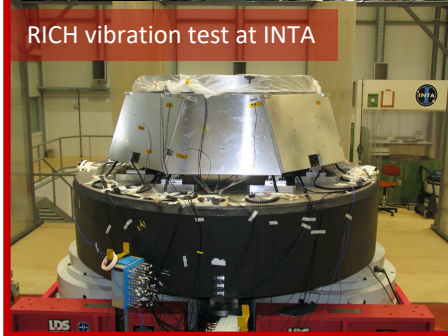
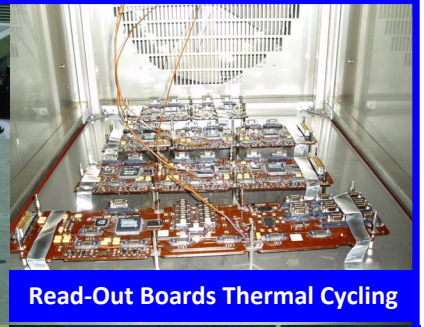
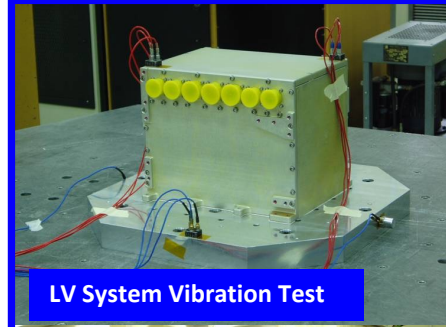
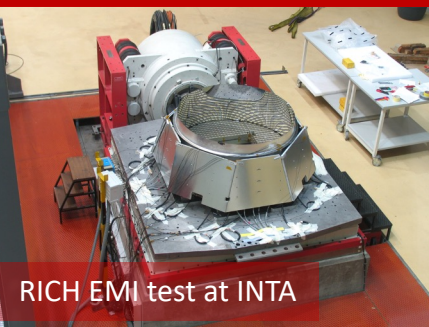
Conical Reflector

3 sectors of Multilayer Structure deposited on a Carbon Fiber Reinforced Composite (CFRC) Substrate



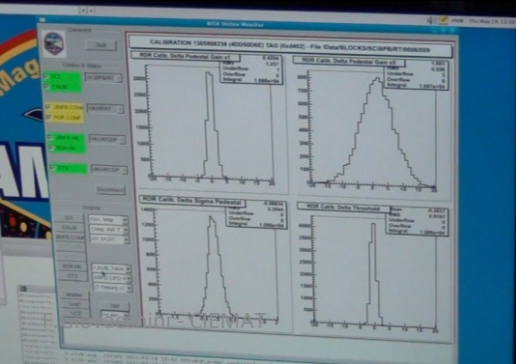
Structure:	Carbon Fiber with epoxy resin
Reflecting surface:	100 nm of Aluminum- Nickel Plated with 300 nm SiO_2 coating
Reflectivity:	$\geq 85 \%$ (at $\lambda = 420 \text{ nm}$)
Roughness:	$\leq 15 \text{ nm}$

The AMS RICH detector: Space Qualification



The AMS-02 RICH: Monitoring & operations

- The detector is continuously running
- RICH critical parameters are constantly monitored 24/7 at CERN AMS Payload Control Center (POCC) to ensure detector integrity and optimal performances
- In >11 years of data taking no major intervention required
- More than 95% of the channels are working properly



RICH 2022



11

RICH Performances on ISS

Response stability

Charge: after temperature corrections the detectors response is stable

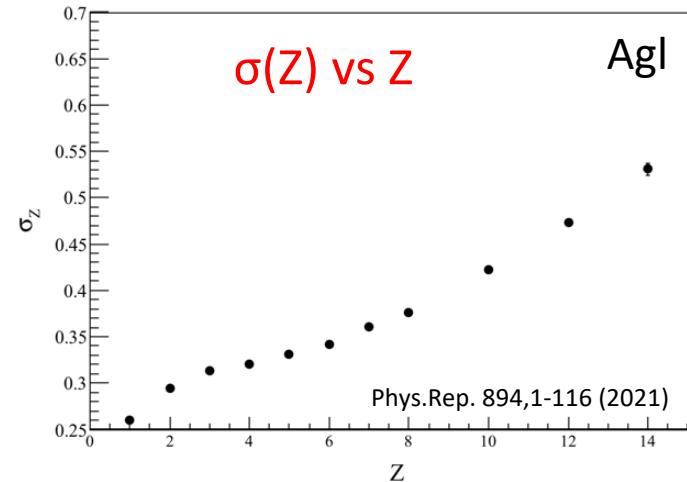
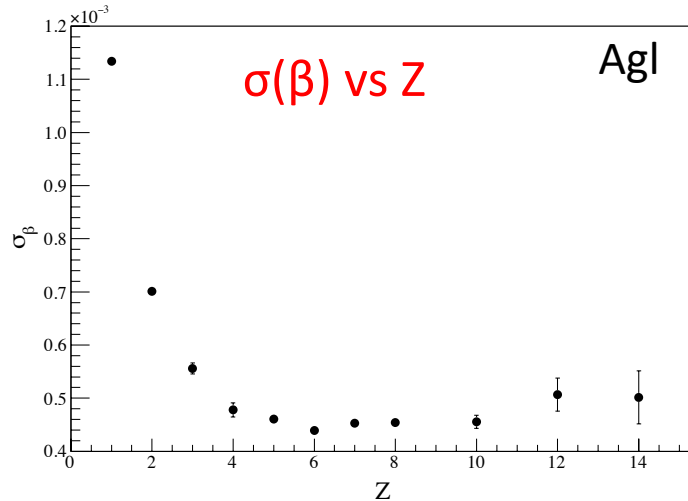
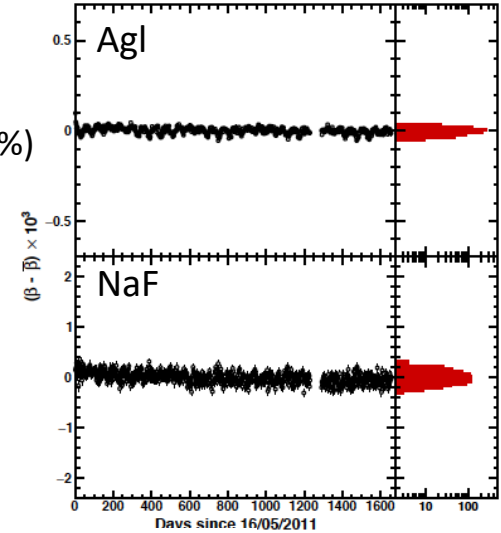
- The residual Photon Yield variation $< 2 \times 10^{-3}$ (95% CL) well within requirements (1%)

Beta: Residual effect on beta are small enough to have no impact in the resolution

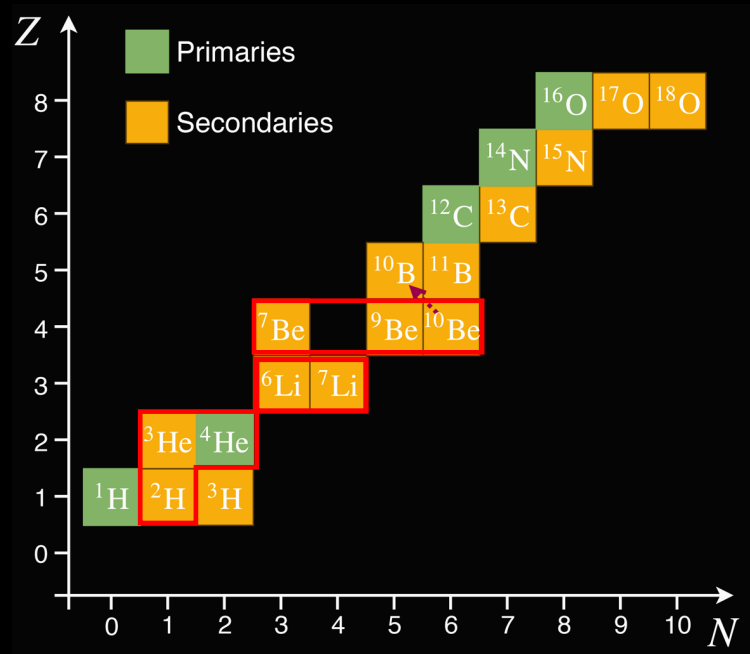
Resolution

Beta: Agl(NaF) resolution ~ 0.7 (1.2) per mil per Helium and better for higher Z

Charge: Resolution ~ 0.3 for Helium

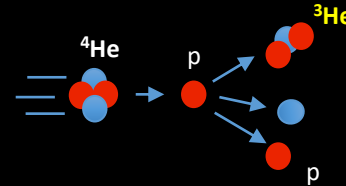
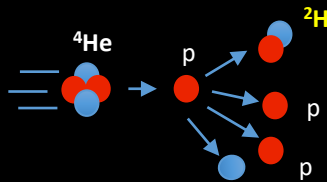


Physics Results: Light Isotopes



Deuterium and Helium Isotopes

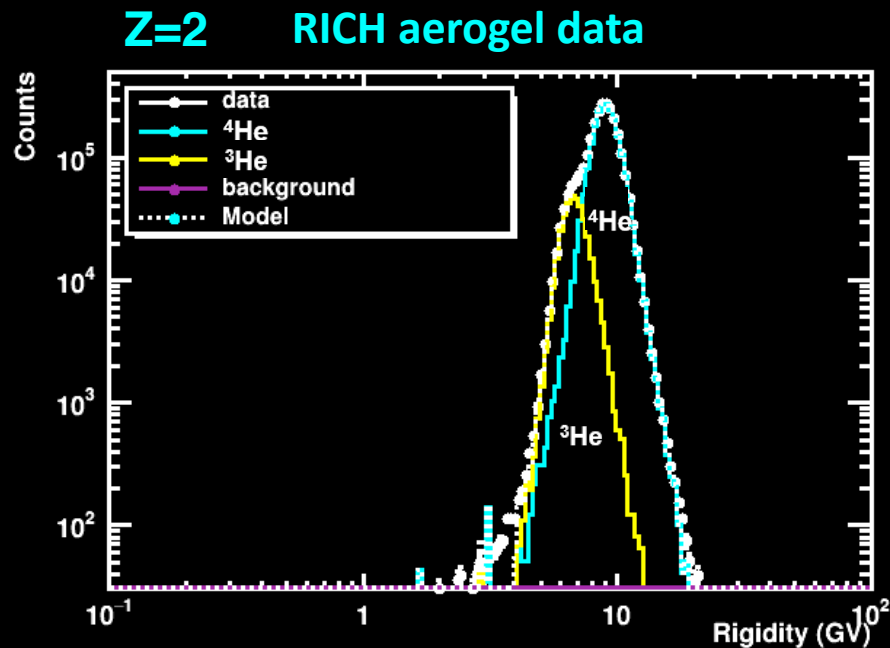
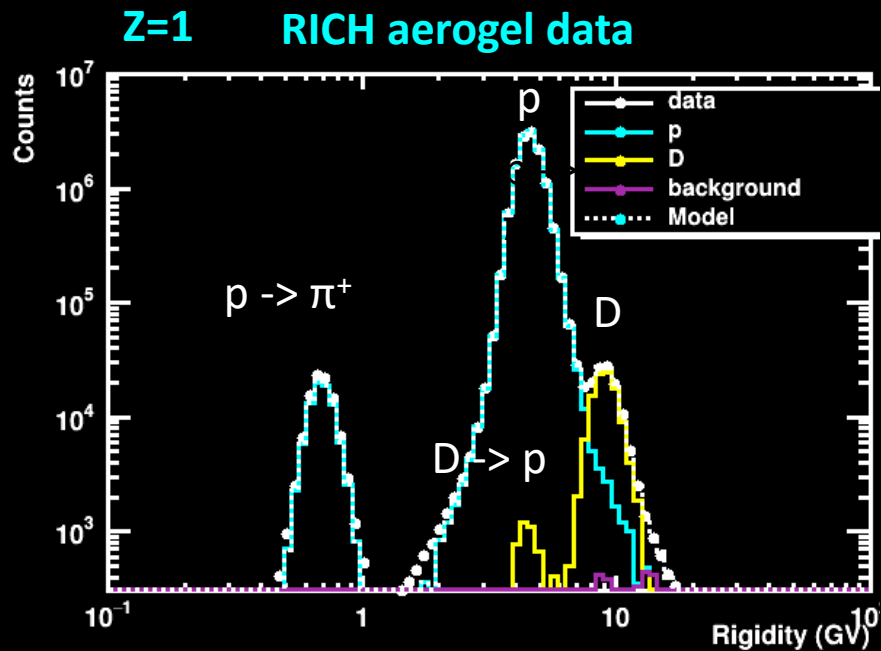
- Helium nuclei are the second most abundant nuclei in cosmic rays.
- ^2H and ^3He are mostly produced by the fragmentation of ^4He : simpler comparison with propagation models than with heavier secondary to primary nuclei ratios.



- The small cross section of He with respect to heavier nuclei, allows $^2\text{H}/^4\text{He}$ and $^3\text{He}/^4\text{He}$ to probe the properties of diffusion at larger distances than any secondary to primary ratio.
- In addition, the different A/Z ratios of ^2H and ^3He allow to disentangle kinetic energy and rigidity dependence of propagation.

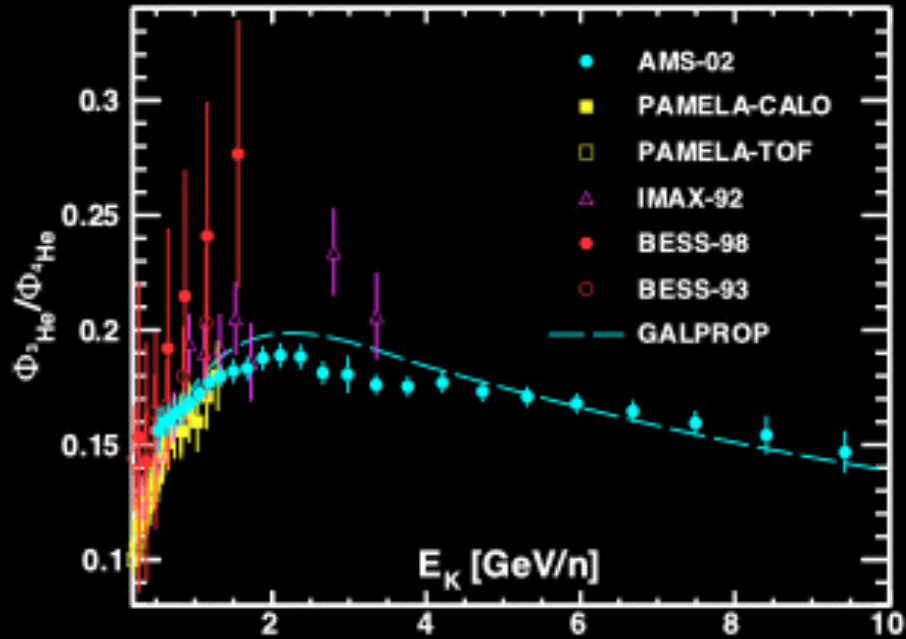
He & H Isotopes identification

Beta \sim 0.985

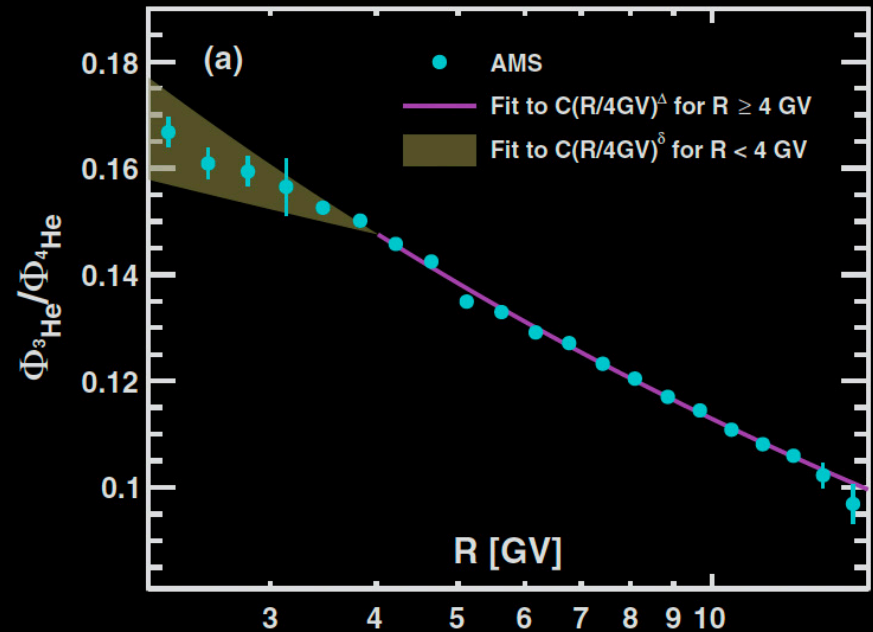


Helium Isotopes Fluxes

PRL 12,181102 (2019) - Editor's suggestion



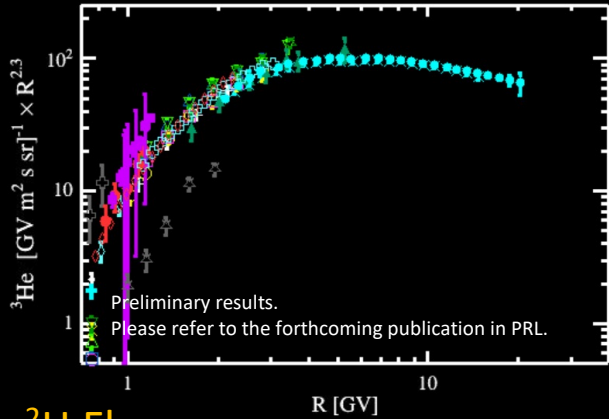
Based on 6.5 years AMS-02 data



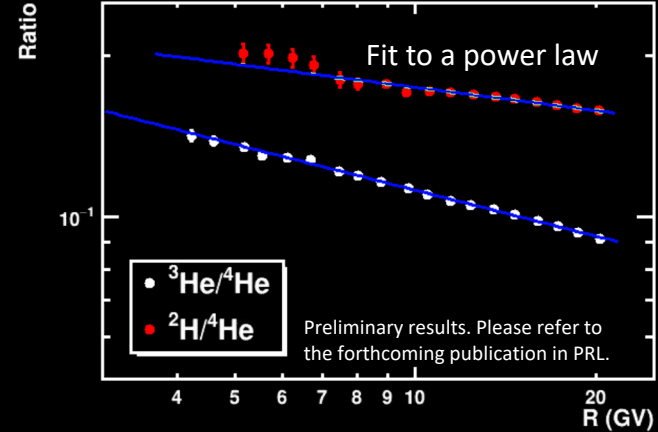
He & H Isotopes Fluxes

based on 10 years AMS-02 data

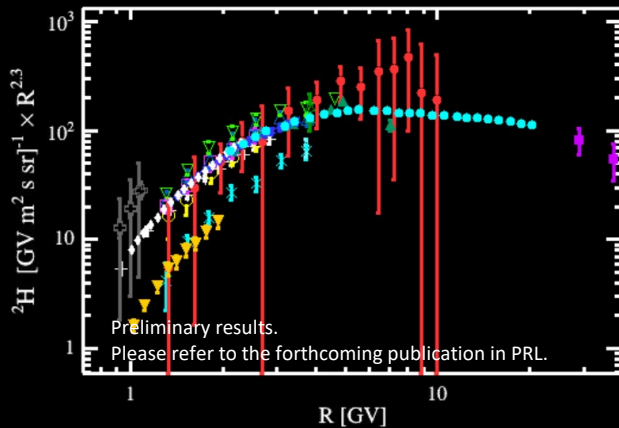
^3He Flux



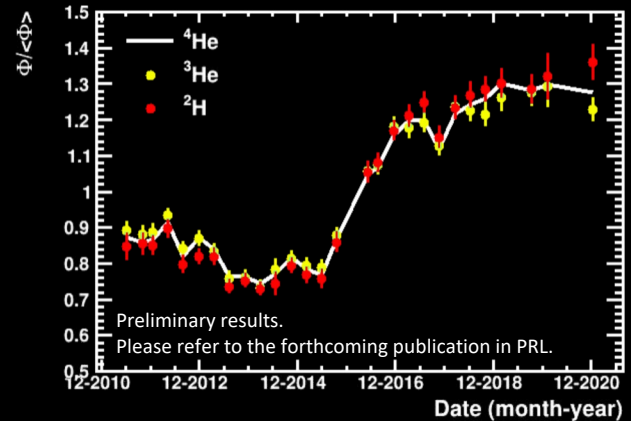
- Err. tot. = $(\text{stat}^2 + \text{syst}^2)^{1/2}$
- + AMS01 (1998/06)
 - × AMS02 (2011/05-2017/11)
 - BESS93 (1993/07)
 - BESS94 (1994/07)
 - △ BESS95 (1995/07)
 - ▽ BESS97 (1997/07)
 - ◇ BESS98 (1998/07)
 - ⊗ Balloon (1965/05)
 - ⊕ Balloon (1966/07+1966/08)
 - Balloon (1973/08)
 - Balloon (1977/07)
 - ▲ IMAX92 (1992/07)
 - ▼ IMP4 (1967/07-1967/10)
 - ◆ IMP7 (1973/05-1973/07)
 - ⊙ ISEE3-MEH (1978/08-1978/12)
 - ⊙ ISEE3-MEH (1979/01-1979/12)
 - ⊙ ISEE3-MEH (1980/01-1980/12)
 - ⊙ ISEE3-MEH (1981/01-1981/12)
 - ⊙ ISEE3-MEH (1982/01-1982/12)
 - ⊙ ISEE3-MEH (1983/01-1983/12)
 - ⊙ ISEE3-MEH (1984/01-1984/12)
 - ⊙ MASS89 (1989/09)
 - ⊙ PAMELA-CALO (2006/07-2007/1)
 - ⊙ PAMELA-TOF (2006/07-2007/12)



^2H Flux



- Err. tot. = $(\text{stat}^2 + \text{syst}^2)^{1/2}$
- + AMS01 (1998/06)
 - × BESS00 (2000/08)
 - BESS93 (1993/07)
 - BESS94 (1994/07)
 - △ BESS95 (1995/07)
 - ▽ BESS97 (1997/07)
 - ◇ Balloon (1975/12)
 - ⊗ Balloon (1977/07)
 - ⊕ Balloon (1990/07)
 - CAPRICE94 (1994/08)
 - CAPRICE98 (1998/05)
 - ▲ IMAX92 (1992/07)
 - ▼ MASS89 (1989/09)
 - ◆ PAMELA-CALO (2006/07-2007/1)
 - ⊙ PAMELA-TOF (2006/07-2007/12)

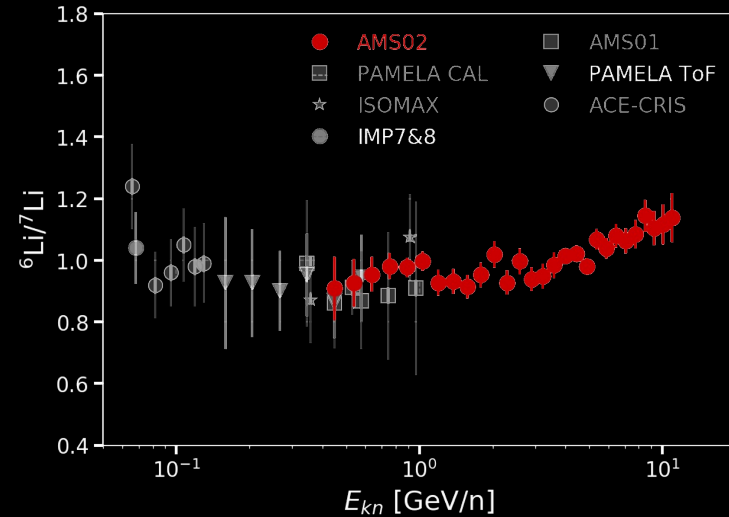
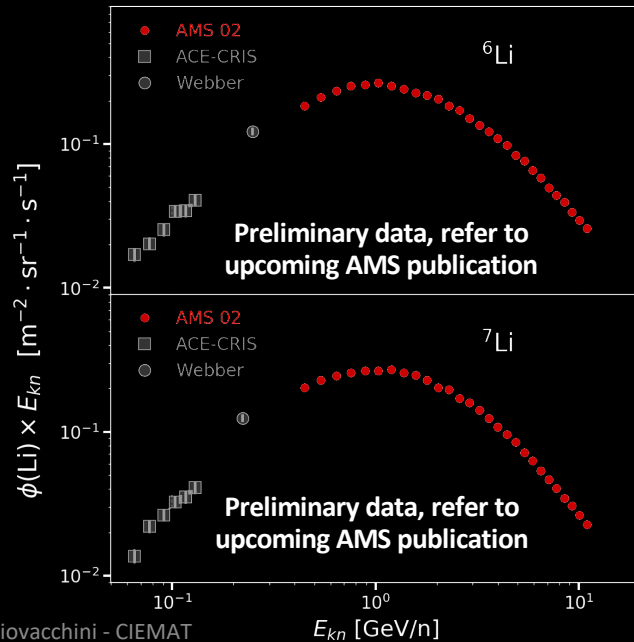


Lithium Isotopes

- Both ${}^6\text{Li}$ and ${}^7\text{Li}$ Secondary produced by the spallation of heavier primary nuclei in CRs.
- Some studies show lithium flux higher than model prediction: Uncertainty in the production cross-section? (Weinrich et al. A&A, 2020); Primary lithium? (Boschini et al. APJ, 2020)

→ First measurement of ${}^6\text{Li}$ and ${}^7\text{Li}$ fluxes above 0.5 GeV/n and up to 12 GeV/n

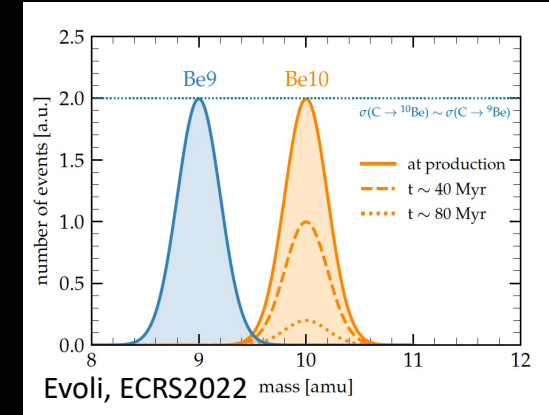
→ Extend the measurement of ${}^6\text{Li}/{}^7\text{Li}$ flux ratio above 1 GeV/n to 12 GeV/n



- Based on 0.8 million lithium events

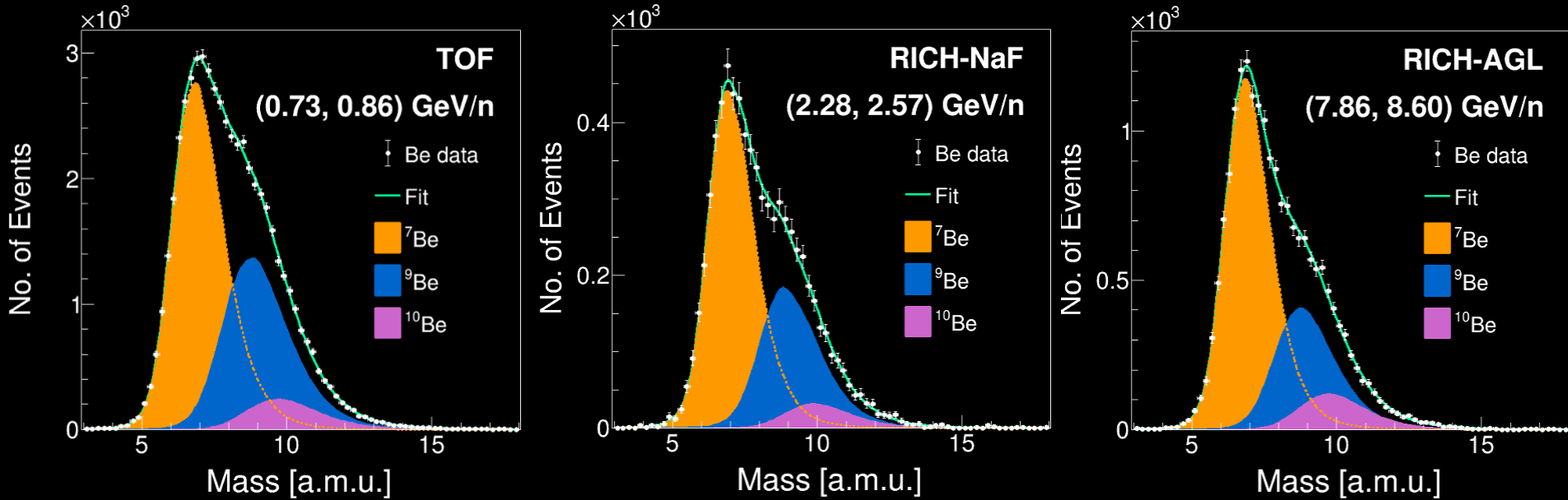
Beryllium Isotopes

- The flux on unstable secondary CRs can be used to constrain the CRs residence time in the galaxy.
- $^{10}\text{Be} \rightarrow ^{10}\text{B}$, $t_{1/2} \approx 1.38 \text{ Myr}$: “radioactive clock”
- Recent studies of cosmic ray propagation using Be/B flux ratio (Evoli et al. PRD, 2020, Weinrich et al. A&A, 2020)



➤ $^{10}\text{Be}/^9\text{Be}$ provides more sensitive measurement of the age of cosmic rays.

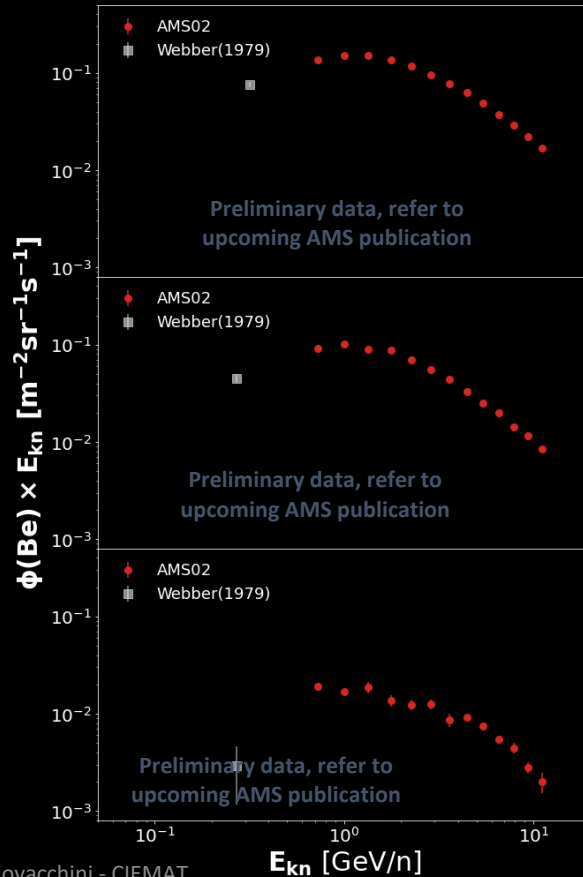
Be Isotopes identification



- Isotopic abundances obtained from mass template fit carried out in difference energy ranges.
- Mass templates are based on Monte Carlo simulation validated by data.

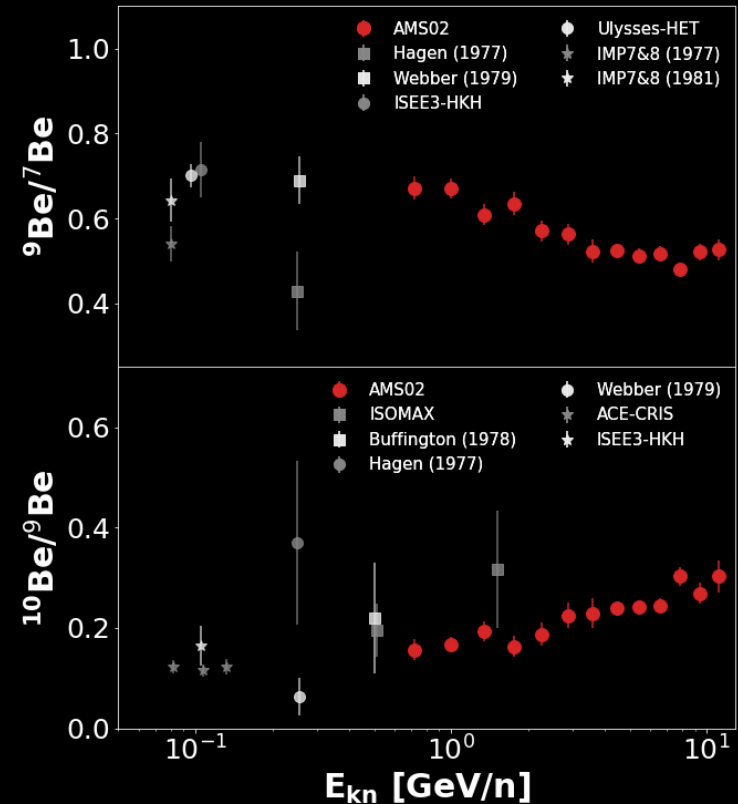
Beryllium Isotopes Fluxes and ratios

→ First measurement of ^7Be , ^9Be and ^{10}Be fluxes above 0.5 GeV/n and up to 12 GeV/n.



→ First measurement of:

- $^9\text{Be}/^7\text{Be}$ flux ratios above 0.5 GeV/n.
- $^{10}\text{Be}/^9\text{Be}$ flux ratios above 2 GeV/n.



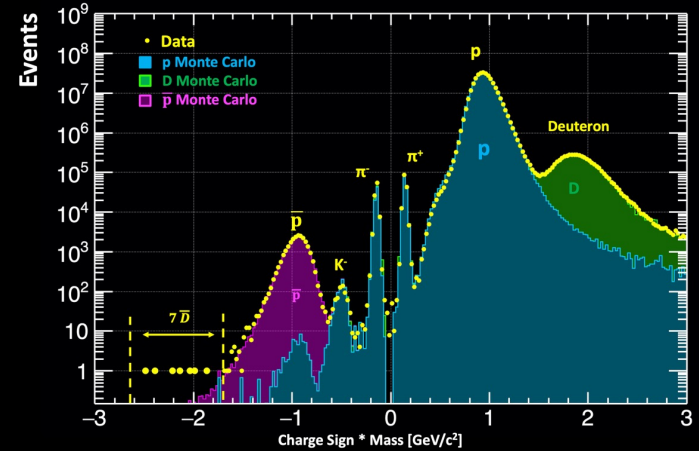
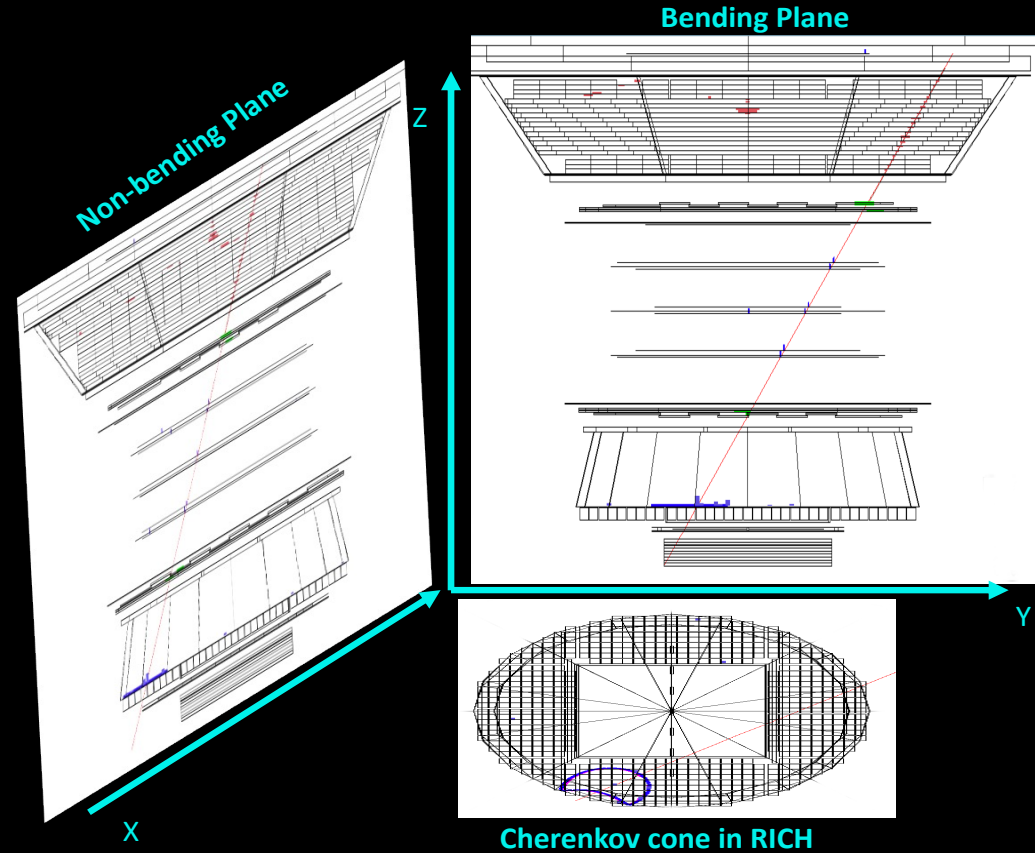
The AMS-RICH detector is successfully taking data since more than 10 years is space aboard the International Space Station proving great contribution to AMS physics!



Search for Light anti-matter

BONUS TRACK

Search for Anti-D candidates

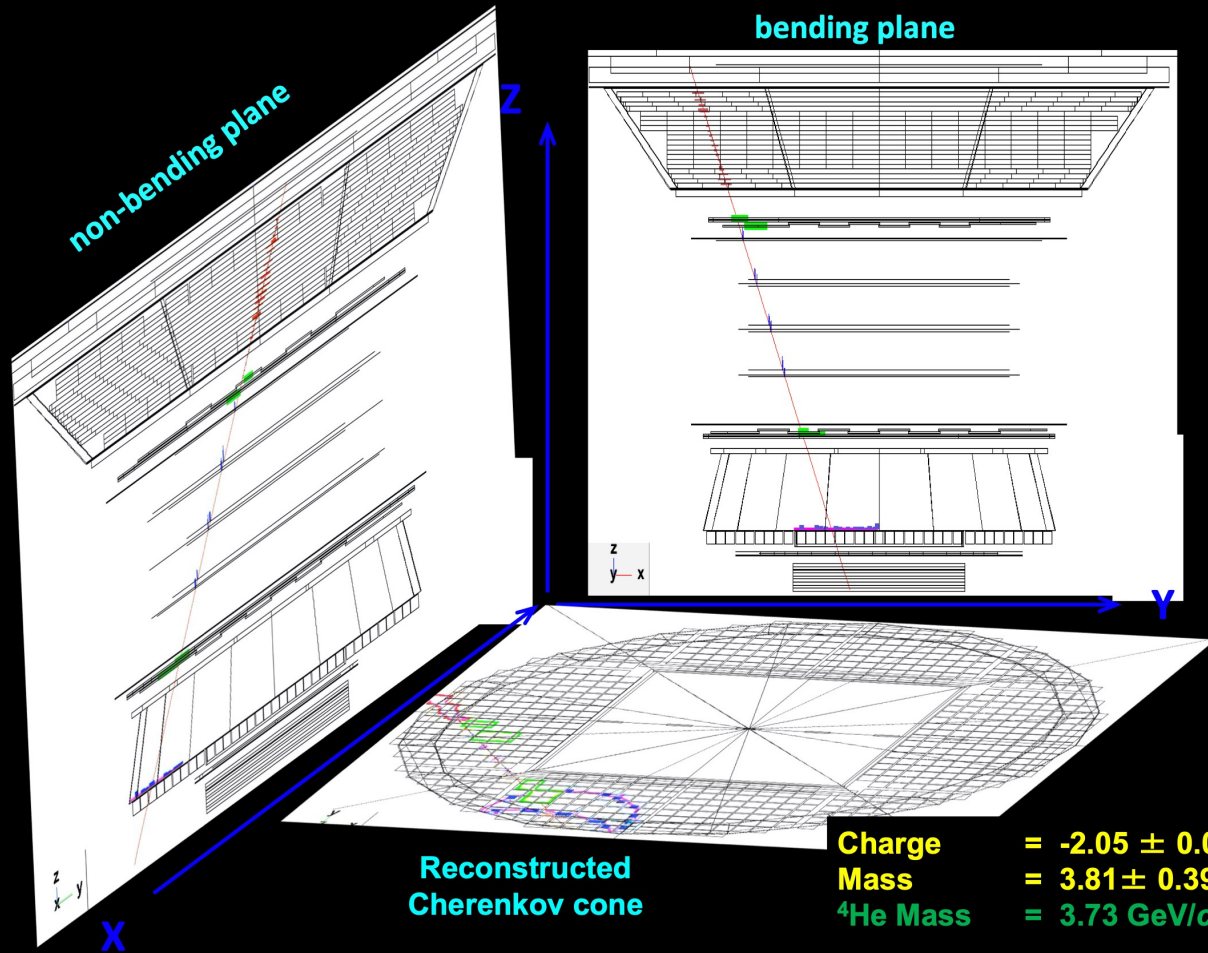


A few antideuteron candidates were selected. Extensive study of the Monte Carlo simulation is on-going to understand the detector effects.

Benefit from continuous data taking through the lifetime of the Space Station

Anti-deuteron Candidate
Charge = -1.02 ± 0.05
Mass = $1.9 \pm 0.1 \text{ GeV}/c^2$

Search for Anti-He candidates

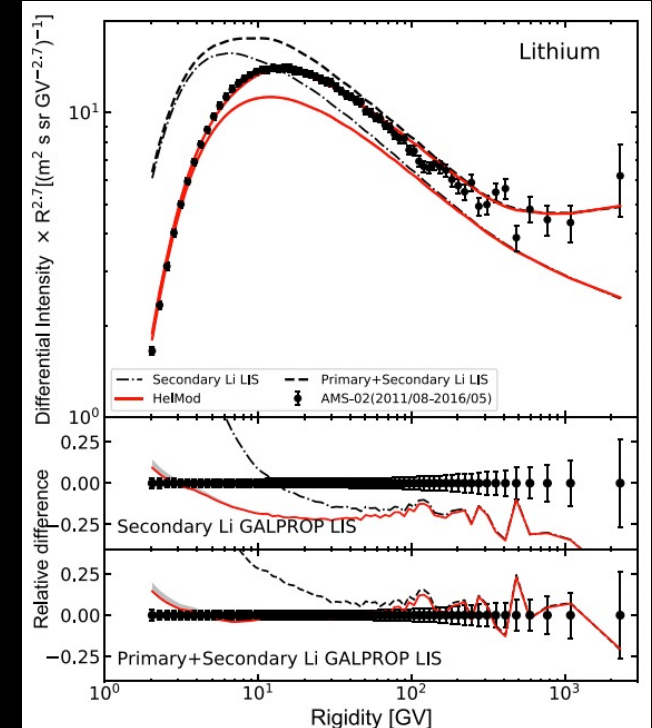


- Few anti-helium candidates were observed with $R < 50 \text{ GV}$;
 - All masses are in the ^3He or ^4He mass ranges ;
 - 1 anti-He in about 100 million helium;
 - No bg expected by MC;
 - At this level MC simulation are difficult to validate.
- Increase acceptance with L)0 upgrade (300%)

Lithium Isotopes

- Both ${}^6\text{Li}$ and ${}^7\text{Li}$ Secondary produced by the spallation of heavier primary nuclei in CRs.
- Some studies show lithium flux higher than model prediction: Uncertainty in the production cross-section? (Weinrich et al. A&A, 2020); Primary lithium? (Boschini et al. APJ, 2020)
- Studies of lithium isotopic composition may help to investigate the mechanism.

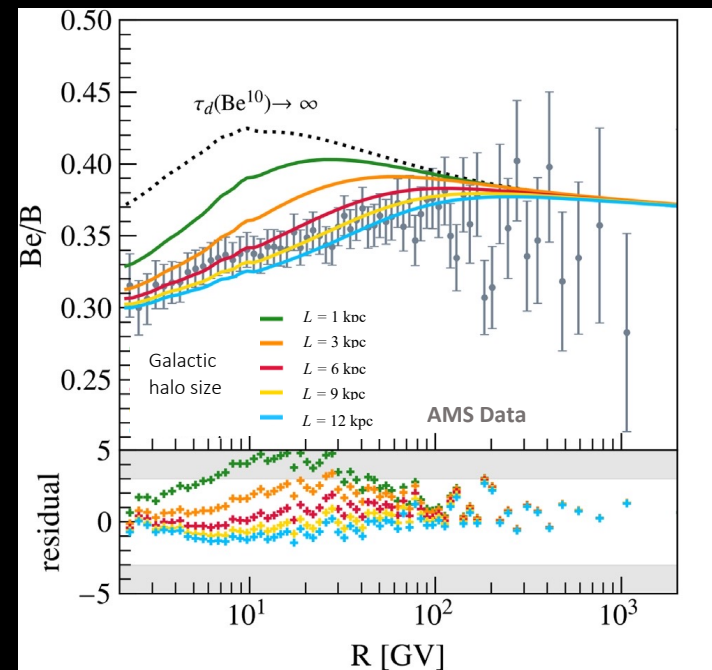
Boschini et al. APJ, 2020



Beryllium Isotopes

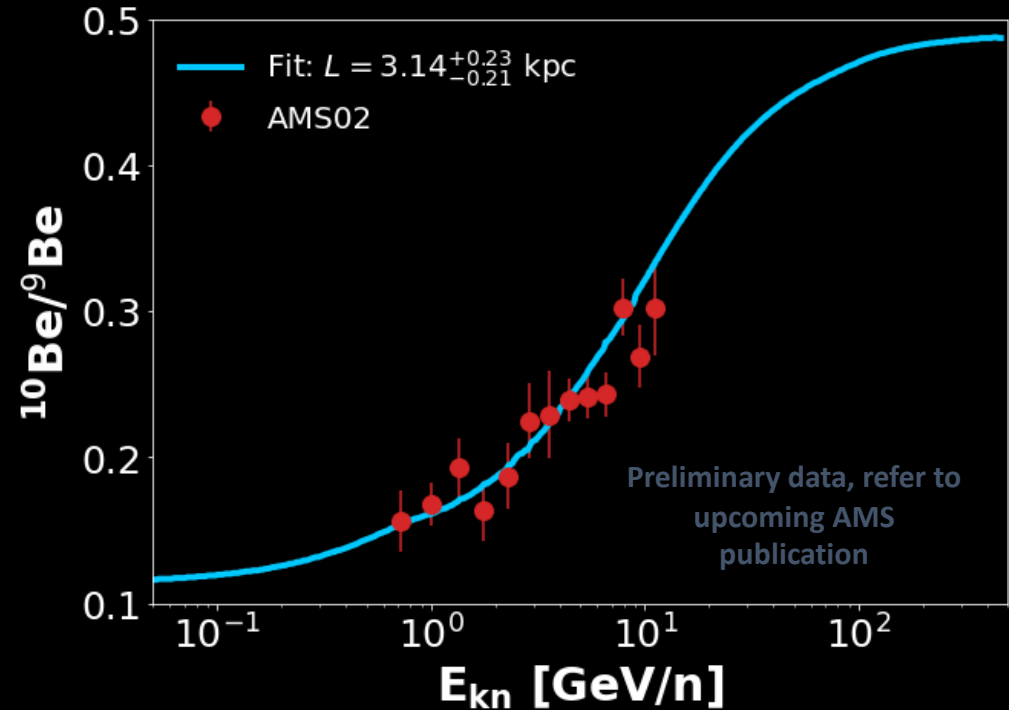
- The flux on unstable secondary CRs can be used to constrain the CRs residence time in the galaxy.
- $^{10}\text{Be} \rightarrow ^{10}\text{B}$, $t_{1/2} \approx 1.38 \text{ My}$: “radioactive clock”
- Recent studies of cosmic ray propagation using Be/B flux ratio:
 - Evoli et al. PRD, 2020
 - Weinrich et al. A&A, 2020
- $^{10}\text{Be}/^9\text{Be}$ provides more sensitive measurement of the age of cosmic rays.

Evoli et al. PRD, 2020



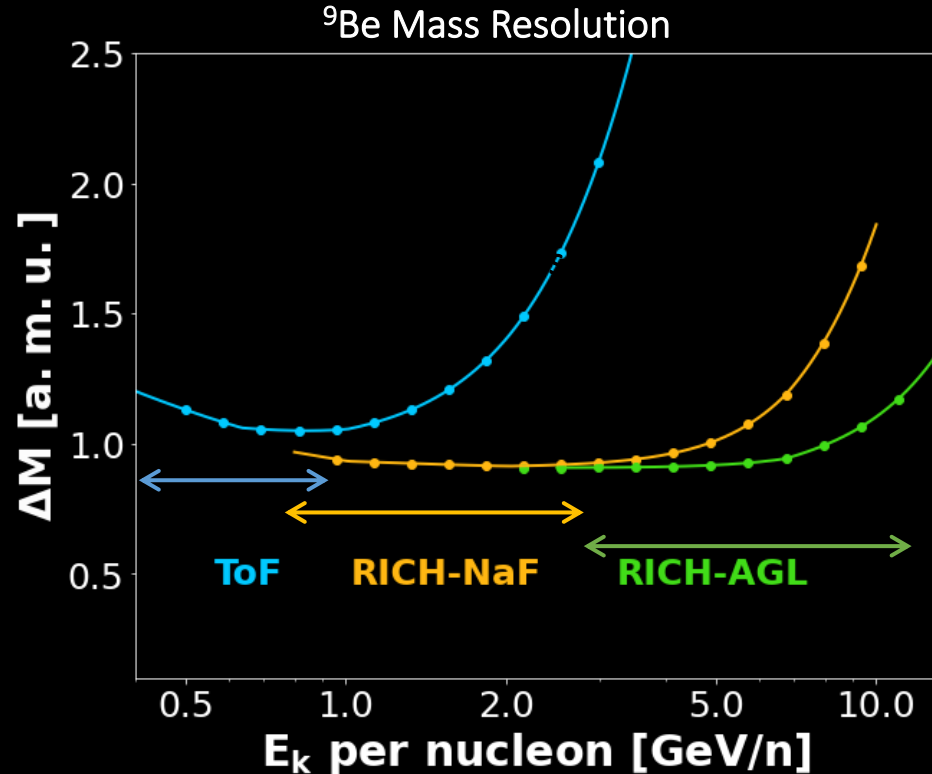
Fitting the $^{10}\text{Be}/^9\text{Be}$ Flux Ratios

- Galactic diffusion halo size L fitted on AMS02 data with an analytical formula:
(D. Maurin *et al.*, arXiv:2203.07265)
- Precision on L from AMS02 data**
 $\Delta L_{\text{AMS02}} \sim 0.2$ kpc.
- Error dominated by uncertainty from production cross-section (1 kpc).



Be Isotopes identification

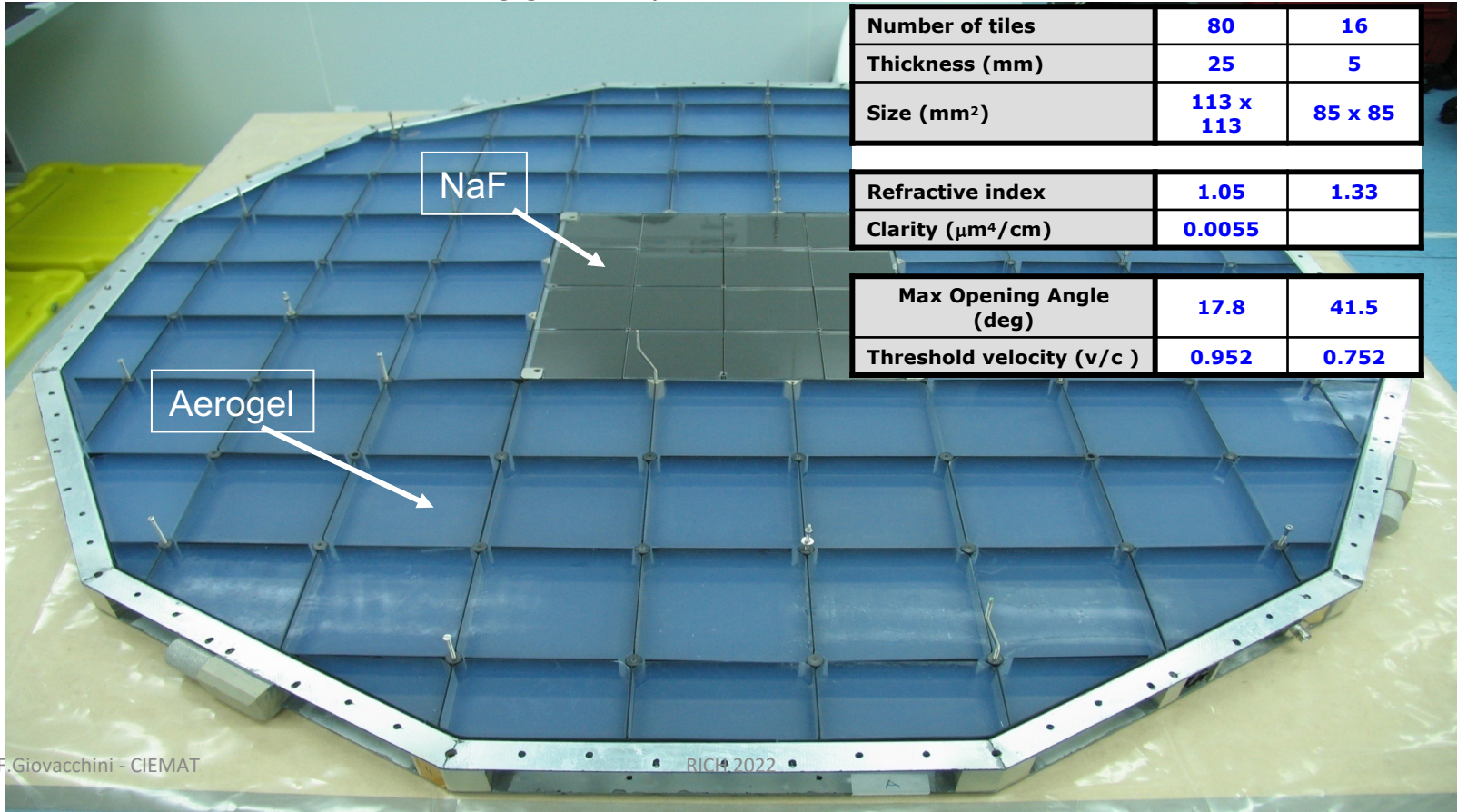
$$\frac{\Delta M}{M} = \sqrt{\left(\frac{\Delta R}{R}\right)^2 + \left(\gamma^2 \frac{\Delta\beta}{\beta}\right)^2}$$



$\Delta M \sim 1$ a.m.u. \rightarrow Unable to do event-by-event isotope identification

Radiator: Structure & Container

- The tiles are enclosed inside a sealed carbon fibre structure.
- A set of inlet and outlet valves equipped with filters allows the vent-out and vent-in of the container for launch and landing.
- Container is filled with N₂ during ground operations.



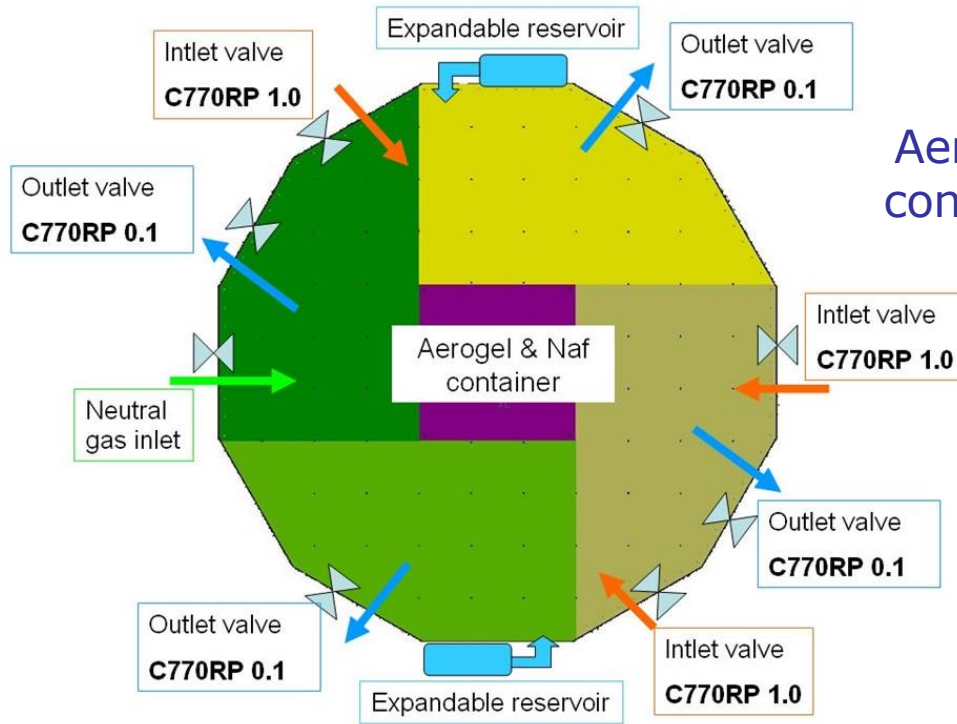
	Aerogel	NaF
--	---------	-----

Number of tiles	80	16
Thickness (mm)	25	5
Size (mm ²)	113 x 113	85 x 85

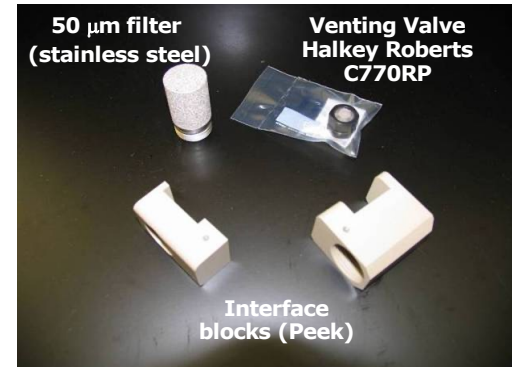
Refractive index	1.05	1.33
Clarity (μm ⁴ /cm)	0.0055	

Max Opening Angle (deg)	17.8	41.5
Threshold velocity (v/c)	0.952	0.752

Radiator: Venting



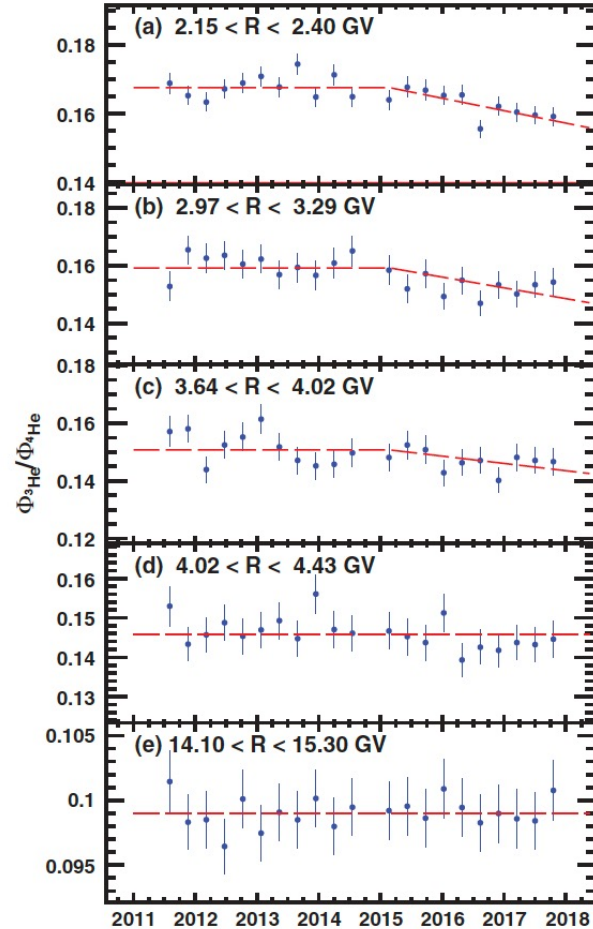
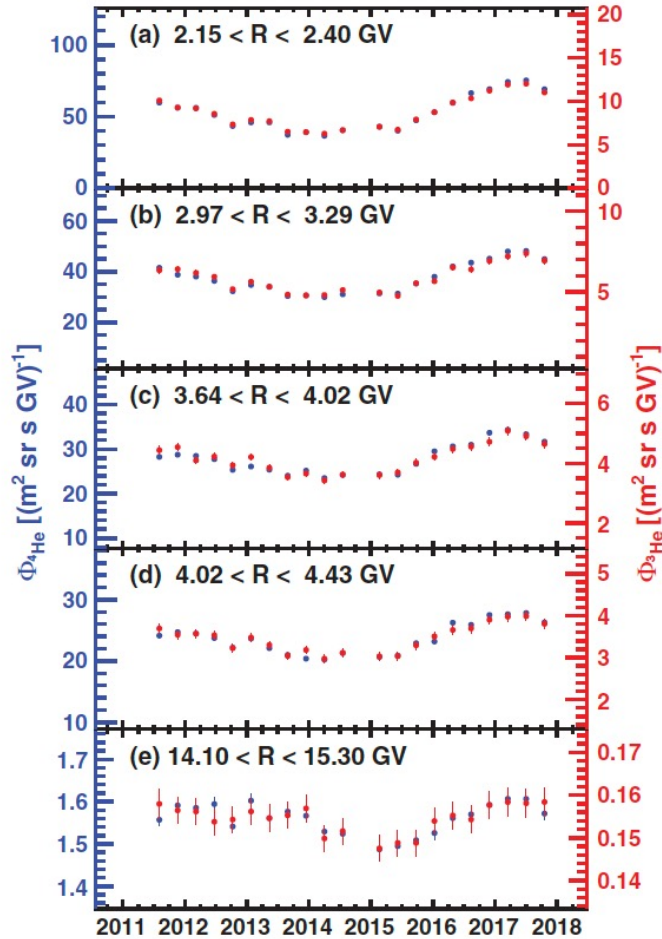
Aerogel and NaF require a controlled dry environment



Container filled with neutral gas (Nitrogen) whenever not in dry atmosphere

- compensates atmospheric pressure variations
- Launch/landing venting capability

PRL 12,181102 (2019) - Editor's suggestion



e
t
t
t
c
r
f
e
t
c
4
t
l
l
e
r